STM Studies of Electron Transfer Through Single Molecules at Electrode-Electrolyte Interfaces

Richard J. Nichols,

The Department of Chemistry, The University of Liverpool, Liverpool L69 7ZD, United Kingdom.

nichols@liverpool.ac.uk

Abstract

Electrochemical scanning tunnelling microscopy (EC-STM) is one of the most important tools in modern interfacial electrochemistry. Over several decades it has proven its worth by providing in-situ atomic and molecular scale visualisations of electrode surfaces, but its value goes far beyond topographic imaging. This article discusses the use of EC-STM as a tool for quantitatively studying mechanisms of electron transfer (ET) at electrode-electrolyte interfaces. In combination with theoretical modelling, it has been revealing mechanistic details of charge transfer across molecules at electrochemical interfaces which are of broad interest to a wide range of electrochemists. This article discusses different ways in which the EC-STM can be deployed to monitor charge flow through single molecules and thereby analyse ET mechanisms. Mechanisms covered range from superexchange to 2-step hopping ones such as the Kuznetsov Ulstrup (KU) mechanism. Literature examples of a variety of redox and non-redox molecular targets are used to describe how measurements of single molecule conductance as a function of electrode potential can be used to analyse charge transfer through single molecules. The review finishes by highlighting some of the most recent work and new developments which will ensure that EC-STM will continue to be an important tool for studying ET mechanisms at electrode-electrolyte interfaces.

Keywords: Scanning tunnelling microscopy, electron transfer, molecular electronics, single molecule conductance, electrochemical gating.

1.1 Introduction

The scanning tunnelling microscope (STM) was invented in the early 1980s with the scientific community being astounded by the ultra-high resolution of surfaces which could be attained. Binnig and Rohrer shared the Noble Prize for Physics in 1986 for this design achievement, together with Ruska "for his fundamental work in electron optics, and for the design of the first electron microscope".[1, 2] The STM had swift impact in surface science with its ability to produce atomic scale real space images of conducting surfaces under ultra-high vacuum and ambient environments. It was relatively quickly realised that STM could operate with atomic resolution in water[3] or an electrolyte and from the late 1980s the technique started to be adopted by electrochemical groups worldwide.[4-8] Since the STM tip forms an additional electrode in the electrolyte environment the STM had to be adapted to a 4-electrode configuration (working, reference, counter and STM tip as a second working electrode) with bi-potentiostat control. In order to reduce faradaic leakage current to the electrolyte all but the very apex of the STM tip had to be isolated with an insulating coating.[9] With these adaptations early studies showed that atomic resolution could be obtained of single crystals and adsorbates under well controlled electrochemical conditions. A selection of high-resolution images obtained under electrochemical conditions are shown in Figure 1. These illustrate the diversity of adsorbate structures which can be imaged with atomic or molecular resolution electrochemical STM, including adsorbed anions (A),[10] organic monolayers (B),[11] metal underpotential metal deposits (C),[12] and even enzymes (D) [13]. Since these early studies, there have been a great diversity of imaging studies under defined electrochemical conditions and the technology has been advanced to study

electrode surface dynamics with video rate STM imaging.[14] These imaging studies showed that the STM could be operated with great stability and precise control of the electrode potentials of both the STM tip and the substrate, a prerequisite for studying charge transfer across molecules at the electrode-electrolyte interface which is the focus of this review.

In the earlier stages of electrochemical STM the overwhelming experimental emphasis was in using the method to image surfaces and adsorbates at high resolution, examples of which are shown in Figure 1. Together with the use of single crystal electrochemistry the high resolution afforded by STM enabled a great deal of new understanding, including details of electrode potential dependence of molecular and ion adsorption, surface structure and reconstruction and fundamental studies of metal underpotential and bulk deposition, electrocatalytic processes, film formation and corrosion. However, as STM relies on the flow of electrons between the STM tip and the substrate surface it can also be used to *quantitatively* study the effect of electrode potential on current flow through molecules at the electrochemical interface. This has proven to be a very valuable modern tool for studying mechanisms and devising models for charge flow through single molecules at electrochemical interfaces as detailed in this review.

There are two general schemes in which electron transfer through molecules can be studied with the electrochemical STM. The first one is the electrochemical scanning tunnelling spectroscopy implementation (EC-STS). Here the STM tip is held above a molecular adsorbate on the electrode surface and the tunnelling current passing from the STM tip through the molecule to the electrode surface can be monitored as a function of the electrode potential and other conditions. The second scheme is termed here the “wired molecular junction” (WMJ). Here the molecule is attached between the surface and the STM

tip and the current flow through this “wired” molecular junction can be studied under electrochemical control. These respective methods are described in the next section.

2.1 Methods for Single Molecule Electrolyte Gating

With its ability to place a metal tip with sub-nanometre precision close to a substrate surface the STM technique is an outstanding tool for forming single molecule junctions. For electrochemically controlled experiments two general variants of STM techniques have been used to form “wired” molecular junctions. Both techniques use the STM tip to form the junction, but they differ in the way the junction is formed. In the *I*(*s*) (*I* = current and *s* = distance) technique the STM tip is approached close to the substrate which is covered by a monolayer or sub-monolayer of the target molecule.[15] This initial approach, which is followed by retraction of the STM tip, is illustrated in Figure 2. This very close approach can lead to stochastic formation of junctions (A to B in Figure 2). The central panel in Figure 2 shows the junction conductance versus retraction distance for a case where a molecular bridge forms (upper curve with plateau) and where no bridge forms (lower curve with the exponential decay). At point B the junction conductance is high as the tip to substrate distance is small. As the tip is retracted from B to C the conductance through the molecular bridge drops and a conductance plateau develops as the distance expands from C to D. On further tip retraction the conductance drops abruptly, as a result of the molecular junction breaking at either the metal-molecule contact or because of cleavage of metal-metal bonds of the contact. This cycle of molecular junction formation and cleavage is repeated many times to accumulate many conductance-distance curves which are then presented in histograms, examples of which are shown in this review.

The *I*(*s*) method described above can be referred to as a “non-contact” method in the sense that the STM tip does not physically touch the substrate surface during the many approach-

retraction cycles.[15, 16] The STM break junction (STM-BJ) technique is a closely related method in which similar approach-retraction cycles are applied but molecular junction formation is preceded by a metal-metal contact formation and breaking processes (hence the term "break junction").[17] The retraction cycles are then characterised by high conductance steps as the metal-metal contact cleaves, followed by lower conductance steps as the metal-molecule-metal junction cleaves. In the case of Au-Au contacts the high conductance steps are at G_0 (~77 mS) or multiples thereof. In this case G_0 is the conductance of gold atom single point contacts.[17] Although the *I*(*s*) and STM-BJ techniques are closely related they have their respective advantages and disadvantages. The STM-BJ technique generally produces a higher "hit rate", which is the probability that any cycle leads to the formation of a molecular junction rather than an "empty" junction. On the other hand, as the *I*(*s*) method does not indent the substrate surface it can maintain analysis on flat surface areas. This is useful where the tip and substrate are different materials, for example a metal STM tip with semiconducting or graphene[18] substrates, for example. Several other techniques have been used less commonly for single molecule conductance characterisation under electrochemical conditions. The mechanically controlled break junction (MCBJ) is a widely used method in molecular electronics. In this method an ultra-thin metal wire bridge can be repeatedly broken and reformed in opening and closing cycles, with molecules being captured in the break junction during the opening phase. The metal bridge is usually suspended on a flexible substrate which can be bent with ultra-high precision and stability. Electrochemical cells can be built around this platform facilitating electrochemical gating of junction conductance.[19-21] Another method is the STM *I*(*t*) method[22] which is related to the *I*(*s*) method described above. As in the *I*(*s*) method molecular bridges between the STM tip and substrate form when the tip is brought very

close to the substrate in a similar manner to A→B in Figure 2. However, in the *I*(*t*) technique (*I*=current, *t* = time) the tip is not retracted and as it is kept at a constant distance current jumps can be seen as single molecular junctions form and break.[22] All of the aforementioned technique can be adapted to a "hold and voltage sweep" mode. In such modes junctions are formed and transiently held at a certain extension and either current versus bias voltage or current versus electrode potential sweeps are rapidly acquired. Illustrative example of such an approach can be found in reference [23], for example.

The aforementioned techniques all probe current flow between "wired" molecular junctions of the form metal|molecule|metal. Generally, the molecular target has anchoring groups, such as thiols or amines, at each respective end so that a molecular bridge robustly spans between the contacts as illustrated in Figure 2. An alternative approach is to use the STM to probe current flow through molecules which are only attached to the substrate. This is the electrochemical scanning tunnelling spectroscopy (EC-STS) approach which also provides a powerful platform for studying single-molecule junction electronic conductivity at electrode-electrolyte interfaces. This approach was first used for detailed single molecule electrochemical spectroscopy by N.J. Tao,[24] who studied how current flow through porphyrins at graphite-electrolyte interfaces was modulated by the electrode potential. The concept of EC-STS is illustrated in Figure 3 for this example.

3.1 Mechanisms of Electrolyte Gating

3.1.1 Tunnelling Mechanisms

Tunnelling is generally the principal charge transport mechanism for short molecular bridges (nanometre or sub-nanometre lengths), with relatively large HOMO-LUMO gaps and frontier orbitals separated from the Fermi level energies of contact electrodes. As the molecular bridge gets longer, or as its molecular levels align closer to the metal electrode Fermi

energies, hopping mechanisms may then come into play as described in the following section. Note that for coherent tunnelling mechanisms molecular levels do not become populated during the charge transfer between the contacting electrodes. There are many models for tunnelling through barriers considering diverse barrier shapes, energetics, bias voltages, and barrier dimensionalities. The simplest barrier models are one-dimensional rectangular barriers, as deployed in the Simmons model,[25] and triangular or trapezoidal barriers. A useful parameter for assessing the conductance decay with barrier width or molecular length (L) is the decay constant β. This can be assessed by measuring the barrier conductance as a function of barrier width, for example for a series of oligomers to give the relationship:

$$G = G_C e^{-\beta L} \qquad \text{Equation 1}$$

With respect to this tunnelling equation, for molecular bridges under electrochemical control the electrode potential could change the decay of conductance with length, β, or the contact conductance G_C. Here, it is more instructive to consider the Landauer formular representation of coherent tunnelling through metal-molecule-metal junctions. This formular is for the conductance by tunnelling through metal-molecule-metal junctions.

$$G = \frac{2e^2}{h}.\Gamma_L.\Gamma_B.\Gamma_R \qquad \text{Equation 2}$$

This is an expression for coherent tunnelling through a single channel, where *h* is Planck's constant, *e* is the charge on an electron and the Γ terms are transmission coefficients relating respectively to the left contact (L), the molecular bridge (B) and the right contact (R). For charge transport by coherent tunnelling through a molecular bridge the electrode potential can tune any or all of these coupling terms or transmission coefficients. The product of these transmission coefficients, $\Gamma_L.\Gamma_B.\Gamma_R$, is the complete junction transmission

coefficient and this can be computed by quantum mechanical methods, for example using density functional theory (DFT) combined with non-equilibrium Green's function formalisms. The conductance can then be calculated by integrating $T(E)$ across the relevant energy window. The impact of electrode potential or changes in molecular bridge redox state on transmission coefficients can also be modelled, by introducing charge onto the molecular junction counterbalanced by ions placed in immediate proximity. Dipolar solvent molecules can also be introduced to surround ("solvate") molecular bridges in such models and can be orientated to gate the junction conductance.[26] However, it should be noted that changes in electrode potential or electrochemical charging of molecular bridges may shift the charge transport regime from tunnelling to other mechanisms such as incoherent sequential charge transport.

Figure 4A is an illustration of coherent tunnelling through a molecular bridge between a metal substrate and STM tip, whose Fermi level energies are separated by the applied bias voltage, eV_{bias}. Frontier molecular orbital corresponding to HOMO and LUMO states are marked in this illustration, and since these are relatively far away from the contact Fermi energies the tunnelling can be described as "mid-gap", i.e. far from resonance. The centre of the panel sketches out the transmission function, which for this example is lowest in the mid-gap. The electrode potential can be used to tune the gap between a frontier molecular orbital and contact Fermi energies, as is described in section 4.1.1. On the other hand, tunnelling transport through molecular bridges may also be described as "resonant" when electronic states on the molecular bridge are tuned by either the bias voltage or the electrode potential to be resonant with the Fermi levels of the metal electrode contacts. Resonant electron transfer through a redox centre centred between two electrodes is illustrated in Figure 4B. Here Gerischer's formulism is used to represent the distribution of

empty oxidised (D_{ox}) and occupied reduced (D_{red}) states.[27] The reorganisation energy (λ) and potential of the redox couple (E_{redox}) are marked on this illustration. The distribution of the oxidised state takes on a Gaussian form, with ε being the energy of the oxidised state in solution, η is the overpotential, k_B is the Boltzmann constant and T the temperature.[27]

$$D_{ox}(\epsilon, \eta) = c\left[\frac{\pi}{4\lambda kT}\right]^{1/2} exp\left[-\frac{(\lambda-\epsilon+e_0\eta)^2}{4\lambda k_B T}\right] \qquad \text{Equation 3}$$

(D_{red}) has a similar form with numerator in the exponential changing to $-(\lambda + \epsilon - e_0\eta)^2$. Importantly, both D_{ox} and D_{red} have maxima energetically shifted away from E_{redox}. The maximum tunnelling current is achieved at resonance when either the maximum in D_{ox} or the maximum in D_{red} are aligned with the central value between the Fermi level energies of the tip and substrate. This corresponds to resonance tunnelling through the oxidised or reduced molecular states. This has been modelled by Schmickler using concepts from Marcus theory.[28, 29] The tunnelling current for resonant tunnelling through the oxidised state in given by the integral in the energy window between the two metal electrode Fermi energies[29]:

$$i \propto \int_0^r D_{ox}(\varepsilon - e_0\eta + V_{bias})\,.\,d\varepsilon \qquad \text{Equation 4}$$

Since the maximum in D_{ox} is shifted from E_{redox} by the reorganisation energy (λ) the maximum resonance current is not achieved at the redox potential. On the contrary the maximum current from resonant tunnelling through the oxidised state occurs at the following electrode potential $\phi_0 - \lambda - V_{bias}/2$, where ϕ_0 is the equilibrium potential, and the half the bias voltage (V_{bias}) is taken as dropping at the redox site centred in the junction.

3.1.2 Sequential Charge Transport Models

In contrast to the tunnelling models described above, charge can sequentially transfer through the molecular bridge as it flows between the two metal contacts. In this case the

redox active bridge molecule is sequentially reduced and oxidised (or oxidised and reduced) as electrons (or holes) hop from one contact to the other. There are then clear connections to electron transfer in molecular electrochemistry. For electron transfer from the substrate to STM tip through an oxidised molecular state, the rates of electron transfer from the substrate to the oxidised redox group ($k^{r/o}$) and from the reduced group to the tip ($k^{o/r}$) are akin to electrochemical charge transfer rates. Since the mechanism is now sequential and charge resides temporarily on the redox centre, there will also be dynamics associated with reorganisation and relaxation at the redox centre, prior to and following the electron transfer steps. These rates depend on whether there is weak coupling between the redox groups and enclosing electrodes or whether there is strong electronic coupling. For strong electronic coupling (adiabatic limit) the respective rates are[30]:

$$k^{o/r} \approx \frac{\omega_{eff}}{2\pi} exp\left[-\frac{[\lambda - e\eta - \gamma eV_{bias}]^2}{4\lambda k_B T}\right]$$

$$k^{r/o} \approx \frac{\omega_{eff}}{2\pi} exp\left[-\frac{[\lambda + e\eta - (1-\gamma)eV_{bias}]^2}{4\lambda k_B T}\right] \qquad \text{Equation 5}$$

While for the weak coupling limit there are additional pre-exponential terms in the electron transfer rate equations[30-33]:

$$k^{o/r} \approx 8\kappa_{tip}\rho_{tip}k_B T \frac{\omega_{eff}}{2\pi} exp\left[-\frac{[\lambda - e\eta - \gamma eV_{bias}]^2}{4\lambda k_B T}\right]$$

$$k^{r/o} \approx 8\kappa_{subst}\rho_{subst}k_B T \frac{\omega_{eff}}{2\pi} exp\left[-\frac{[\lambda + e\eta - (1-\gamma)eV_{bias}]^2}{4\lambda k_B T}\right] \qquad \text{Equation 6}$$

Where κ is the electronic transmission coefficient for the electron transfer, ρ the metallic electron density, ω_{eff} is a characteristic nuclear vibrational energy, γ is the fraction of the bias voltage experienced at the redox site, η is the electrochemical overpotential and other terms are as defined previously.

These rate constants can be used to formulate the current flow across the molecular bridge for the two respective limits, weak and strong coupling. For weak coupling this gives[30]:

$$i_{tunn}^{weak} = e\frac{k^{o/r}k^{r/o}}{k^{o/r}+k^{r/o}} \qquad \text{Equation 7}$$

On the other hand when the coupling is strong[30, 33]:

$$i_{tunn}^{strong} = 2en_{o/r}\frac{k^{o/r}k^{r/o}}{k^{o/r}+k^{r/o}} \qquad \text{Equation 8}$$

The term $n_{o/r}$, which is present when there are strong electronic interactions between the molecular redox group and the electrodes, has important implications. In this adiabatic limit, following pre-organisation through environmental fluctuations and the first electron transfer step by a Franck-Condon transition, the vibrationally excited redox centre proceeds to relax. However, during the relaxation a cascade of electrons, quantified as $n_{o/r}$ in this equation, can continue to transfer over as the relaxation proceeds. The term $n_{o/r}$ can be seen as amplifying the current from the 2-step sequential charge transfer process in the adiabatic limit, while for the weak coupling limit there is full relaxation following the transfer of a single electron.

Both the weak and strong coupling limits feature maximum junction current at the equilibrium potential for the redox centre, which readily distinguishes these sequential charge transfer mechanisms from resonant tunnelling. The strong coupling limit is quantitatively expressed in the Kuznetsov-Ulstrup (KU) equation for the enhanced current ($j_{enhanced}$), where ξ is the fraction of the electrode potential at the redox site and j_0 is a pre-exponential factor which is detailed in reference [34] and other terms are as previously defined:

$$j_{enhanced} \approx j_0 \exp\left(-\lambda/4kT\right)\frac{\exp\left(e|V_{bias}|/4kT\right)}{cosh\left(\frac{e(0.5-\gamma)V_{bias}-e\xi\eta}{2kT}\right)} \qquad \text{Equation 9}$$

As will be shown in section 4.2, the KU equation is useful for assessing whether 2-step sequential tunnelling mechanism prevails close to the equilibrium potential, for quantifying reorganisation energies (λ) and the fraction of the electrochemical potential drop

experienced at the redox centre (ξ) and for evaluating electrolyte effects on electron transfer through the molecule.

A final model described in this section is the “soft gating” mechanism also developed by Kuznetsov and Ulstrup.[35] This mode is characterised by large configurational fluctuations of the molecular junction which can dominate the charge transport patterns. The “soft gating” is applied within a superexchange mechanism of charge transport across the molecular bridge. In the superexchange model the molecular bridge is not electrochemically reduced or oxidised, but thermally accessible large configurational fluctuations of the dynamic molecular bridge bring it into non-equilibrium configurations which are favourable for superexchange tunnelling. These gate the conductance as the electrode potential is tuned and this model has been used to rationalise the sigmoidal conductance increase as the electrode potential is shifted negative for viologen molecular bridges in aqueous electrolytes.[35]

This is a very condensed discussion of key models for electron transfer across molecules in an STM nanogap under electrochemical conditions, with a focus on those models which have been applied to the experimental data described below. For more detailed discussions the reader is referred to reference [34] or the detailed book by Kuznetsov and Ulstrup[31].

In the case of DFT computations of tunnelling through molecular bridges there are now a collection of individual studies which have taken different approaches to modelling the influence of electrochemical redox switching or molecular charging, some which include the impact of the electric field, electrolyte or solvent environments.[26, 36-38]

4.1 Experimental Studies

4.1.1 Controlling Phase Coherent Transport Through Electrolyte Gating

The earlier demonstrations of electrolyte gating in single molecule STM junctions involved using the electrode potential to switch the molecular target between different redox states which exhibited pronounced changes in junction conductance.[15, 24, 39-43] Some years later it was demonstrated that electrolyte gating could be used to modulate the conductance of single molecule junctions without oxidising or reducing the molecular bridge.[44, 45] This can be understood most simply by considering Figure 4. The simplest tunnelling molecular bridges between metal electrodes have a LUMO and HOMO resonance separated by a broad gap, as illustrated in that figure. Tunnelling can be mid-gap, as illustrated, or the Fermi level can be aligned closer to the HOMO or LUMO resonances. The first demonstration of electrolyte gating in non-redox molecular bridges was for Au|bipyridine|Au junctions where "bipyridine" refers to 4,4'-bipyridine (44'BPy). This has a relatively small HOMO-LUMO gap when compared to, for example, alkanedithiols, and the Fermi energy is aligned towards the foot of the LUMO resonance. The LUMO resonance can be modelled as a Lorentzian dependent on parameters such as the orbital coupling and molecular resonance position.[45] As the electrode potential is gated negative the conductance increases, as the gold Fermi level position climbs up the tail of the LUMO resonance. Another good example of such electrochemical gating without reduction or oxidation of the molecular bridge is coronene containing molecular wires which consist of 13 fused benzene rings. These also conduct through the tail of the LUMO by tunnelling.[46] Such non-redox electrolyte gating has also been achieved with nickel electrodes, where it has been shown that both the molecular conductance and the electrolyte gating are significantly enhanced compared to gold contacts.[47] Using electrochemical conditions, the nickel electrode and STM tip could both be maintained as oxide free surfaces, in contrast to normal ambient air conditions where nickel surfaces would be covered by oxide layers. This

highlights another advantage for the use of proper electrochemical conditions for such single molecule studies. Figure 5 shows conductance histograms for Ni|44'BPy|Ni and Au|44'BPy|Au single molecule junctions at the marked electrode potentials (applied to the substrate and with V_{Bias} = 0.1 V).[47] The electrode potentials are against a polypyrrole quasi-reference electrode which is a convenient choice for the confined space in an in-situ electrochemical STM cell. The conductance peak is seen to shift with electrode potential in both cases. This shift is plotted in figure 5C for the two systems, where the enhancement of both junction conductance and electrolyte gating with nickel contacts is clear. Here the gate voltage (V_{Gate}) is calculated by assuming that V_{Gate} = 0 corresponds to the potential of zero charge (PZC) of the given electrode. The enhanced electrolyte gating with Ni electrode contacts can be attributed to several factors. The pyridyl anchoring group has a stronger binding with Ni due to stronger hybridisation of the Ni d-electrons with adsorbate frontier molecular orbitals. The gating mechanism is also fundamentally different for Ni where spin degeneracy of the charge transport is lifted due to the ferromagnetic properties of the Ni contacts. Here it is the contribution of the minority spin channel which dominates the behaviour around E_F to give peaks in the transmission function which are sufficient close to the LUMO resonance; these peaks are absent for the majority spin channel. These peaks correspond to hybridisation of the LUMO of 44'BPy with the minority spin channel of the Ni electrodes. Negative electrolyte gate voltages then bring E_F closer to the LUMO resonance and increases these peaks due to hybridisation and thereby boosts the conductance. This shows how single molecule electrochemical STM measurements combined with theory can be used to help to understand spin polarised charge transport at ferromagnetic metal electrodes.[47] A subsequent study, which also used Ni contacts in an electrochemical STM-BJ setup, showed that the conductance of 4,4'-vinylenedipyridine (44VDP) depends on both

the electrochemically applied gate voltage and the pH of the electrolyte. Here discrete proton transfers to and from a single 44VDP molecular bridge under electrochemical potential control significantly modulated the STM junction conductance.[48]

The preceding examples demonstrate electrolyte gating for tunnelling in the vicinity of a transport resonance where the electrode potential tunes the metal contact Fermi energies in the tail of the transport resonance, without any redox change occurring in the molecule. For the model example sketched in Figure 4 and also 44'BPy with gold contacts the transmission function is relatively straightforward with the gap between the LUMO and HOMO resonance being featureless. On the other hand, spin-polarisation has a major impact when the Au contacts are substituted for Ni ones in the 44'BPy system, with additional spin dependent charge transmission peaks in the region of E_F impacting on the junction electrical characteristics as described above. Molecular bridges featuring quantum interference can also be used to manipulate the junction charge transport characteristics using electrolyte gating. The importance of quantum interference phenomena in charge flow through molecules has been widely recognised in molecular electronics. It has been experimentally studied in single molecule junctions by comparing charge flow through junctions with different connectivity or differing conjugations or bonding topologies; for example, cross conjugation can bring about destructive interference. Such phenomena are clear manifestations of the quantum effects in the passage of electrons through molecular bridges. As an aside the STM has been a very important tool for studying quantum phenomena in nanoscale systems. Here a classic demonstration of the wave like nature of electrons confined within nanoscale structures was elegantly visualised by Eigler.[49] This experiment involved the STM imaging of the (square of the) "electron wavefunction" of surface electron confined with a ring 48 Fe atoms on a copper single crystal. This "quantum

corral" experiment imaged the interference pattern of the surface confined electronic wave which appeared in the STM image like ripples caused by a stone thrown into a pond. Electrons and hence current flowing across molecular bridges are also subject to quantum interference as the waves traverse multifarious possible trajectories concurrently. A propaedeutic example is current flow across a benzene ring with a hypothetical pair of metal electrode contacts placed either meta or para to each other. Transport is mid-gap here and quantum interference is between the HOMO and LUMO frontier molecule orbitals. Current flow between the 1→4 (para) sites is enhanced compared to the destructive quantum interference between the 1→3 (meta) sites. Why this is the case is explained in an instructive manner by Tada and Yoshizawa with orbital rules.[50] The orbital phases at the respective ring positions determine whether interference is destructive or constructive. The zeroth order Green's function for propagation of tunnelling electrons at the Fermi energy between sites, r and s, on the benzene ring is written as two terms, the first one representing the contribution of the HOMO and second one the LUMO:

$$\frac{C_{r\mathrm{HOMO}}C_{s\mathrm{HOMO}}*}{E_F-\varepsilon_{\mathrm{HOMO}}} - \frac{C_{r\mathrm{LUMO}}C_{s\mathrm{LUMO}}*}{E_F-\varepsilon_{\mathrm{LUMO}}} \qquad \text{Equation 10}$$

Since the transport is as at the Fermi energy placed midway between the LUMO and HOMO, the denominator in the first term is positive, while it is negative in the second term. The respective orbital phases appearing in the numerator are then determining. For para junctions the sign of $C_{1\mathrm{HOMO}}C_{4\mathrm{HOMO}}$ is negative while $C_{1\mathrm{LUMO}}C_{4\mathrm{LUMO}}$ is positive, and hence the two terms in this equation co-add to non-zero values (constructive). On the other hand, for meta junctions (1->3 connectivity) both these terms have the same sign and the two terms in Equation 10 cancel, producing destructive interference.[50]

For the preceding paragraph it is clear that quantum interference adds structure to the "gap" region of the transmission functions of non-redox molecular junctions, for example

effective destructive quantum interference can produce sharp and deep valleys in transmission curves. For two terminal junctions the alignment of the contact Fermi levels is generally in a relatively fixed position with respect to such dips. However, electrolyte gating provides the opportunity to tune to such dips, or in the case of constructive QI to transmission (or conductance) peaks. Since transmission (or conductance) versus E_F can be computed by ab-initio methods and E_F can be transcribed to the given reference electrode scale, such QI phenomena can be effectively predicted and modelled for phase coherent tunnelling.

Several publications have exploited QI features with the tuning of electrochemical gating potential. [21, 36, 51-54] An illustrative example is shown in Figure 6 in which the electrochemical gating of terphenyl molecular wires with iodine anchoring termini is achieved.[54] Here the para and meta analogues are compared. These give quite different conductance versus electrochemical gate voltage profiles (Figure 6c). The meta wire shows a sharp dip in conductance which occurs when the electrode potential is tuned to the quantum interference feature.[54]

4.1.2 Redox Electrolyte Gating

Mechanistically, redox electrolyte gating poses more complexity than the non-redox electrolyte gating presented in the former section. While non-redox gating has been shown in all cases to date to fit phase coherent transport models, this is not the case for redox electrolyte gating, where different systems have been shown to exhibit phase coherent tunnelling, resonant tunnelling or incoherent charge transfer mechanisms including hopping type models. A variety of redox active molecular junctions have been studied under electrochemical control or electrochemical actuation including viologens, [15, 35, 41, 55-62] tetrathiafulvalene (TTF) derivatives and analogues,[21, 57] substituted

perylenetetracarboxylic diimides (PTCDI) and naphthalene diimide, [23, 63-69] quinones/ anthraquinones[36, 51, 70-73], aniline, polypyrrole and other oligomers,[40, 74-77] fullerenes containing molecular wires,[78] -NO_2 substituted oligo(phenylene ethynylene) (OPEs),[79, 80] benzodifuran,[81] metallo-enzymes and DNA,[82-91] and a diverse variety of metal coordination complexes.[24, 39, 42, 43, 92-102] Rather than exhaustively discussing all these examples this section presents a few illustrative examples with discussion of the mechanistic implications.

Figure 7 shows data recorded for a viologen molecular bridge between gold contacts under electrochemical control.[61] Figure 7A illustrates the viologen molecular bridge (called "6V6") in the electrochemical STM setup connected between the 2 gold contacts which form the 2 working electrodes. The reference and counter electrodes in the electrochemical STM cell are also illustrated. Figure 7B illustrates the viologen (V^{2+}) redox active moiety surrounded by electrolyte ions, which in this experiment can be reduced to its radical cation ($V^{+\bullet}$) through electrolyte gating. This electrolyte gating is highly dependent on the type of electrolyte as shown in the respective single molecule conductance data for an ionic liquid electrolyte (Figure 7C) and an aqueous electrolyte (Figure 7D).[61] The solid line in Figure 7C shows the good fit to the Kuznetsov Ulstrup (KU) mechanism for two-step electrochemical charge transport across the redox bridge. The modelling is for 2-step sequential charge transfer in the adiabatic limit. The relative sharpness of the profile attests to the efficient electrolyte gate coupling in the ionic liquid environment. A gate coupling parameter, ξ, of unity is obtained meaning that the applied electrochemical potential is fully experienced at the viologen centre in the molecular bridge. By contrast for the aqueous electrolyte data a much broader profile is apparent which gives a much lower gate coupling parameter of 0.2 for this aqueous gating system with the same viologen (6V6) molecular bridge. In summary,

these data define the mechanism of charge transport for this system as a “hopping” through the redox site, show the impact of the electrolyte environment and enable a quantitative modelling of parameters such as reorganisation energy and fraction of electrochemical potential (and the bias voltage) dropped at the redox site.[61]

Redox gating has also been demonstrated in the electrochemical scanning tunnelling spectroscopy configuration. As highlighted in section 2.1 a classic example here is the work of N.J. Tao who imaged iron (III) protoporphyrin (FePP) complexes with electrochemical STM on a highly oriented pyrolytic graphite (HOPG) substrate.[24] The apparent height of the complex increased near to the electrochemical reduction potential of FePP controlled by tuning the electrode potential. This enhancement in tunnelling current was interpreted as resulting from electrochemical tuning of the Fermi level of the HOPG electrode to align with the lowest unoccupied molecular orbital (LUMO) of FePP.[24] This showed how energy levels could be moved in and out of resonance by adjusting the electrode potential. A resonant tunnelling model was used to explain tunnelling current enhancement close to the reversible potential.

The electrochemical scanning tunnelling spectroscopy configuration has also been used by Albrecht and Ulstrup et al. to analyse electron transfer mechanisms for a variety of redox active molecular monolayers, on noble metal electrode surfaces.[42, 43, 94-96] An instructive example here involves transition metal complexes of osmium and cobalt transition tethered by linking groups to Au(111) or Pt(111) electrodes.[94] This is an interesting comparison since the osmium analogues used exhibited several orders of magnitude faster electrochemical ET kinetics than the cobalt one. Both the osmium and cobalt complexes follow Kuznetsov Ulstrup two-step charge transfer through the redox active metal centre, with maximum STM current enhancement close to the reversible

potential. EC-STS data for $[Os(bpy)_2(p2p)_2]^{2+/3+}$ monolayers on Au(111) in 0.1 M $HClO_4$ are shown in Figure 8.[43] The normalised STM tunnelling current is plotted against overpotential, giving a bell-shaped curve which is slightly displaced from the reversible potential. This is fitted to the Kuznetsov Ulstrup two step model with partial vibrational relaxation. From this fitting quantitative parameters relating to this ET mechanism are obtained, with a reorganisation energy of 0.3 eV and the fraction of the electrode potential experienced at the site of the redox centre of 0.9.[43] This means the effect of the electrode potential is nearly fully felt by the redox centre. On the other hand, the fraction of the bias voltage experienced at the redox site is about 1,[43] implying that the bias voltage is very asymmetrically displaced in the STM gap, since a value of 0.5 would be expected for central placement of redox site in the nanogap. This is not surprising as the molecule is covalently attached to only one of the gold electrodes. This is a notable contrast to the fully "wired" viologen bridge described above in which the molecular bridge is covalently "wired" to both tip and substrate, which usually gives a symmetric placement of the redox moiety in the nano-junction.

There are notable differences between the Os and Co complexes which have important implications for the mechanism of the electron transfer.[94] For the osmium complexes studied the data fits a two-step model with partial vibrational relaxation. A cobalt complex examined in the same study also fitted a two-step model, but in this case with full vibrational relaxation. This reflects the relatively slow electrochemical ET of the Co system. Here two-step ET is in the weak coupling, fully diabatic limit, with the centre and its environment first reorganising so that ET can occur, with then the system fully relaxing and the subsequent electron transfer to the other contact.[94] In the adiabatic limit of the Os system many electrons can transfer ("hop") through the molecular complex for every

environmental preorganisation. This gives rise strong current amplification near to the reversible potential in the EC-STS in Figure 8.[43] By contrast much weaker current amplification was apparent for the Co complex due to its much slower electrochemical ET kinetics.[94]

The examples highlighted above show electrochemical gating either when the molecule is reduced (e.g. the viologens) or oxidised (e.g. ferrocenes). It is also possible for a given molecular junction to exhibit both, which has been referred to as ambipolar.[23, 103] These collected examples of redox electrochemical gating illustrate the level of detail that can be acquired about ET mechanisms through redox active single molecules using the EC-STM in either the EC-STS or "wired" molecular junction mode. The next section highlighting some important developments which give new opportunities for using the EC-STM in single molecule studies.

5.1 Conclusions and Outlook

The STM has shown itself to be a powerful tool for studying mechanisms of charge transfer through single molecules at the electrode- electrolyte interface. This is generally achieved using the EC-STS, STM *I*(*s*) or STM-BJ methods. In EC-STS the STM probes tunnelling current flow through the molecular target which is generally only attached to the substrate, while in the STM *I*(*s*) or STM-BJ methods it is attached to both the STM tip and substrate to form a "wired" junction. Both methods have enabling the identification of various charge transport mechanisms, ranging from phase coherent tunnelling, resonant tunnelling, to 2-step electrochemical hopping. Depending on the details of the mechanism, quantitative parameter that can be extracted including single molecule conductance, IV_{bias} profiles, conductance versus electrode potential, reorganisations energies and potential distributions in the nanogap junction. Electrolyte effects have also been identified with pronounced

differences between ionic liquids and aqueous electrolytes identified. Ionic liquids have been particularly well suited for studying molecular conductance across very broad electrode potential windows and across multiple redox states. A recent example of this is shown in figure 9 which illustrates a single molecular wire with an integral polyoxometalate cluster attached between a Au STM tip and substrate through pyridyl anchoring groups.[104] The defined polyoxometalate cluster contains precisely 7 metal atoms (1 Mn and six Mo). The right of this figure shows the single molecular conductance versus electrode potential, with conductance transitions on switching between differing charge states ($2^- \leftrightarrow 3^- \leftrightarrow 4^-$). Notably, these measurements were made a dry ionic liquid enabling the broad potential window to be explored.[104]

Zhou et al. have approached the important question of whether "molecular conductance correlates with electrochemical rate constants?"[105] They studied 3 molecular systems and compared the molecular conductance and electrochemical rate constants. They found that fast electron transfer rate constants, determined electrochemically, correlate with high single molecule conductance determined with the STM-BJ. Their study was limited to molecules that conduct by superexchange (tunnelling) mechanisms. This is an important aspect for further study with larger homologous series of electrochemically active molecular wires. Also given the importance of incoherent charge transfer (hopping) mechanisms in electrochemistry, bio-electrochemistry and long-range charge transport, examining correlations between heterogeneous ET rate constants and molecular conductance in such systems is certainly overdue.

New ways of binding molecules to electrodes will continue to be important, particularly if they lead to junctions with greater stability, higher conductance and less fluxionality. For example, the thiol bond is highly fluxional which can lead to large stochastic current

fluctuations. Higher junction stability and conductance will become more important as new methods are developed to analyse fluctuations in molecular junction current, arising for example for long-lived redox charged junction states (see next paragraph). An example of junction anchoring group "engineering" for electrochemical studies is the substitution of thiol for carbodithioate ($-CS_2^-$) anchoring groups in redox-active benzodifuran molecular junctions.[81] Here, the carbodithioate anchors gave substantially enhanced electrochemical on/off switching ratios and conductance values. Electrochemical reactions have also been exploited to attach molecules strongly within junctions. Here Hines et al. formed direct Au-C covalent bonds in-situ by electrochemically reducing both terminal diazonium moieties on the molecular wire.[106] They showed that the resulting junctions were significantly more stable than conventionally anchored junctions.

Recent work has also been focused on examining dynamic conductance fluctuations in redox active molecular junctions as a function of electrode potential. Li et al. have monitored such fluctuations for ferrocene molecular wires in an STM-BJ and attributed them to electrode potential dependent stochastic switching between redox states of the molecular bridge.[102] They contended that the fluctuations corresponded to individual redox changing events which could be tuned with the electrode potential. Large current fluctuation around reversible potentials have also been seen for organometallic molecular wires consisting of EMACs (extended metal-atom chains) with gold contact anchoring groups on each end.[107] These EMACs are complexes with a one-dimensional metal atom chains supported by both metal–metal and metal–ligand bonds. Given these developments one of the most promising areas for development is the rapid recording of STM tunnelling current data at hundreds or kHz or even MHz.[108] This will give new opportunities to record junction dynamics at these time scales. This might include monitoring the dynamics

of charged junction states. Recently long-lived charged states in room temperature redox-active single molecular junctions have been identified.[109] In the case of two-terminal Au-porphyrin-Au junctions, charged states of the molecular bridge are formed at moderate bias voltages (~1 V). These states have been shown to persist for several seconds. The high conductance and long-lived charged state results from the weak coupling of specific molecular orbitals which open additional incoherent transport pathways. It has been suggested that these long-lived charged states result from the weak coupling of specific molecular orbitals, with this weak coupling enhancing their longevity, changing the energetics of the junction and greatly impacting on current flow.[109] These unexpectedly persistent charged junction states could have important consequences for electrochemical mechanisms of charge transport across nanoscale junctions, electrochemical conductance switching and molecular electronics in general. The development of new fast STM electronics will help in mapping out and understanding such junction dynamics under electrochemical control.

6.1 Acknowledgements

I would like to acknowledge the many highly significant contributions that Professor Jens Ulstrup has made to theoretical and experimental studies of electron transfer in electrochemical and bioelectrochemical systems. I would like also to thank him for our many collaborations which I have found most inspirational.

Funding support is acknowledged from EPSRC (grants EP/M005046/1, EP/M029522/1 and EP/M014169/1) and the Leverhulme Trust (grant RPG-2019-308).

7.1 References

[1] https://www.nobelprize.org/prizes/physics/1986/summary/.

[2] G.K. Binnig, H. Rohrer, C. Gerber, E. Stoll, Real-Space Observation Of The Reconstruction Of Au(100), Surf. Sci., 144 (1984) 321-335.

[3] R. Sonnenfeld, P.K. Hansma, Atomic-Resolution Microscopy In Water, Science, 232 (1986) 211-213.

[4] K. Itaya, E. Tomita, Scanning Tunneling Microscope For Electrochemistry - A New Concept For The Insitu Scanning Tunneling Microscope In Electrolyte-Solutions, Surf. Sci., 201 (1988) L507-L512.

[5] P. Lustenberger, H. Rohrer, R. Christoph, H. Siegenthaler, Scanning Tunneling Microscopy At Potential Controlled Electrode Surfaces In Electrolytic Environment, J. Electroanal. Chem., 243 (1988) 225-235.

[6] J. Wiechers, T. Twomey, D.M. Kolb, R.J. Behm, An Insitu Scanning Tunneling Microscopy Study Of Au(111) With Atomic Scale Resolution, J. Electroanal. Chem., 248 (1988) 451-460.

[7] O.M. Magnussen, J. Hotlos, R.J. Nichols, D.M. Kolb, R.J. Behm, Atomic-Structure Of Cu Adlayers On Au(100) And Au(111) Electrodes Observed By Insitu Scanning Tunneling Microscopy, Phys. Rev. Lett., 64 (1990) 2929-2932.

[8] S.L. Yau, C.M. Vitus, B.C. Schardt, Insitu Scanning Tunneling Microscopy Of Adsorbates On Electrode Surfaces - Images Of The (Square-Root 3 X Square Root3)R30-Degrees-Iodine Adlattice On Platinum(111), J. Am. Chem. Soc., 112 (1990) 3677-3679.

[9] D.M. Kolb, R.J. Nichols, R.J. Behm, The Application Of Scanning Tunneling Microscopy To Electrochemistry, 1992.

[10] M. Kleinert, A. Cuesta, L.A. Kibler, D.M. Kolb, In-situ observation of an ordered sulfate adlayer on Au(100) electrodes, Surf. Sci., 430 (1999) L521-L526.

[11] W.H. Li, W. Haiss, S. Floate, R.J. Nichols, In-situ infrared spectroscopic and scanning tunneling microscopy investigations of the chemisorption phases of uracil, thymine, and 3-methyl uracil on Au(111) electrodes, Langmuir, 15 (1999) 4875-4883.

[12] J. Hotlos, O.M. Magnussen, R.J. Behm, Effect Of Trace Amounts Of Cl- In Cu Underpotential Deposition On Au(111) In Perchlorate Solutions - An In-Situ Scanning-Tunneling-Microscopy Study, Surf. Sci., 335 (1995) 129-144.

[13] A.G. Hansen, A. Boisen, J.U. Nielsen, H. Wackerbarth, I. Chorkendorff, J.E.T. Andersen, J.D. Zhang, J. Ulstrup, Adsorption and interfacial electron transfer of Saccharomyces cerevisiae yeast cytochrome c monolayers on Au(111) electrodes, Langmuir, 19 (2003) 3419-3427.

[14] O.M. Magnussen, L. Zitzler, B. Gleich, M.R. Vogt, R.J. Behm, In-situ atomic-scale studies of the mechanisms and dynamics of metal dissolution by high-speed STM, Electrochim. Acta, 46 (2001) 3725-3733.

[15] W. Haiss, H. van Zalinge, S.J. Higgins, D. Bethell, H. Hobenreich, D.J. Schiffrin, R.J. Nichols, Redox state dependence of single molecule conductivity, J. Am. Chem. Soc., 125 (2003) 15294-15295.

[16] R.J. Nichols, W. Haiss, S.J. Higgins, E. Leary, S. Martin, D. Bethell, The experimental determination of the conductance of single molecules, PCCP, 12 (2010) 2801-2815.

[17] B.Q. Xu, N.J.J. Tao, Measurement of single-molecule resistance by repeated formation of molecular junctions, Science, 301 (2003) 1221-1223.

[18] Q. Zhang, L.L. Liu, S.H. Tao, C.Y. Wang, C.Z. Zhao, C. Gonzalez, Y.J. Dappe, R.J. Nichols, L. Yang, Graphene as a Promising Electrode for Low-Current Attenuation in Nonsymmetric Molecular Junctions, Nano Lett., 16 (2016) 6534-6540.

[19] C. Shu, C.Z. Li, H.X. He, A. Bogozi, J.S. Bunch, N.J. Tao, Fractional conductance quantization in metallic nanoconstrictions under electrochemical potential control, Phys. Rev. Lett., 84 (2000) 5196-5199.

[20] J.-H. Tian, Y. Yang, X.-S. Zhou, B. Schoellhorn, E. Maisonhaute, Z.-B. Chen, F.-Z. Yang, Y. Chen, C. Amatore, B.-W. Mao, Z.-Q. Tian, Electrochemically Assisted Fabrication of Metal Atomic Wires and Molecular Junctions by MCBJ and STM-BJ Methods, Chemphyschem, 11 (2010) 2745-2755.

[21] J. Bai, A. Daaoub, S. Sangtarash, X. Li, Y. Tang, Q. Zou, H. Sadeghi, S. Liu, X. Huang, Z. Tan, J. Liu, Y. Yang, J. Shi, G. Mészáros, W. Chen, C. Lambert, W. Hong, Anti-resonance features of destructive quantum interference in single-molecule thiophene junctions achieved by electrochemical gating, Nature Mater., 18 (2019) 364-369.

[22] W. Haiss, R.J. Nichols, H. van Zalinge, S.J. Higgins, D. Bethell, D.J. Schiffrin, Measurement of single molecule conductivity using the spontaneous formation of molecular wires, PCCP, 6 (2004) 4330-4337.

[23] I. Diez-Perez, Z. Li, S. Guo, C. Madden, H. Huang, Y. Che, X. Yang, L. Zang, N. Tao, Ambipolar Transport in an Electrochemically Gated Single-Molecule Field-Effect Transistor, ACS Nano, 6 (2012) 7044-7052.

[24] N.J. Tao, Probing potential-tuned resonant tunneling through redox molecules with scanning tunneling microscopy, Phys. Rev. Lett., 76 (1996) 4066-4069.

[25] J.G. Simmons, Generalized Formula for Electric Tunnel Effect Between Similar Electrodes Separated by a Thin Insulating Film, Journal of Applied Physics, 34 (1963) 1793-1803.

[26] E. Leary, H. Hobenreich, S.J. Higgins, H. van Zalinge, W. Haiss, R.J. Nichols, C.M. Finch, I. Grace, C.J. Lambert, R. McGrath, J. Smerdon, Single-Molecule Solvation-Shell Sensing, Phys. Rev. Lett., 102 (2009) 086801.

[27] W. Schmickler, Interfacial Electrochemistry, Oxford University Press., (1996).

[28] W. Schmickler, C. Widrig, The Investigation of Redox Reactions with a Scanning Tunneling Microscope - Experimental and Theoretical Aspects, J. Electroanal. Chem., 336 (1992) 213-221.

[29] W. Schmickler, N.J. Tao, Measuring the inverted region of an electron transfer reaction with a scanning tunneling microscope, Electrochim. Acta, 42 (1997) 2809-2815.

[30] J. Zhang, T. Albrecht, Q. Chi, A.M. Kuznetsov, J. Ulstrup, in Bioinorganic Electrochemistry (ed. O. Hammerich and J. Ulstrup), Springer, Netherlands, (2008) 249-302.

[31] A.M. Kuznetsov, J. Ulstrup, Electron Transfer in Chemistry and Biology, An Introduction to the Theory, John Wiley & Sons Ltd, Chichester., (1998).

[32] A.M. Kuznetsov, Charge Transfer in Physics, Chemistry and Biology, Gordon & Breach, Reading., (1995).

[33] R. Nichols, W. Haiss, D. Fernig, H. Zalinge, D. Schiffrin, J. Ulstrup, (eds O. Hammerich and J. Ulstrup), in Bioinorganic Electrochemistry, Springer, Netherlands, 207-247.

[34] J. Zhang, A.M. Kuznetsov, I.G. Medvedev, Q. Chi, T. Albrecht, P.S. Jensen, J. Ulstrup, Single-molecule electron transfer in electrochemical environments, Chem. Rev., 108 (2008) 2737-2791.

[35] W. Haiss, T. Albrecht, H. van Zalinge, S.J. Higgins, D. Bethell, H. Hoebenreich, D.J. Schiffrin, R.J. Nichols, A.M. Kuznetsov, J. Zhang, Q. Chi, J. Ulstrup, Single-molecule conductance of redox molecules in electrochemical scanning tunneling microscopy, J. Phys. Chem. B, 111 (2007) 6703-6712.

[36] M. Baghernejad, X.T. Zhao, K.B. Ornso, M. Fueg, P. Moreno-Garcia, A.V. Rudnev, V. Kaliginedi, S. Vesztergom, C.C. Huang, W.J. Hong, P. Broekmann, T. Wandlowski, K.S. Thygesen, M.R. Bryce, Electrochemical Control of Single-Molecule Conductance by Fermi Level Tuning and Conjugation Switching, J. Am. Chem. Soc., 136 (2014) 17922-17925.

[37] W. Su, J. Jiang, W. Lu, Y. Luo, First-principles study of electrochemical gate-controlled conductance in molecular junctions, Nano Lett., 6 (2006) 2091-2094.

[38] H. Cao, J. Jiang, J. Ma, Y. Luo, Temperature-dependent statistical behavior of single molecular conductance in aqueous solution, J. Am. Chem. Soc., 130 (2008) 6674-6675.

[39] W. Han, E.N. Durantini, T.A. Moore, A.L. Moore, D. Gust, P. Rez, G. Leatherman, G.R. Seely, N. Tao, Lindsay, STM Contrast, Electron-Transfer Chemistry, and Conduction in Molecules, J. Phys. Chem. B, 101 (1997) 10719-10725.

[40] H.X. He, X.L. Li, N.J. Tao, L.A. Nagahara, I. Amlani, R. Tsui, Discrete conductance switching in conducting polymer wires, Phys. Rev. B, 68 (2003) 045302.

[41] W. Haiss, H. van Zalinge, H. Hobenreich, D. Bethell, D.J. Schiffrin, S.J. Higgins, R.J. Nichols, Molecular wire formation from viologen assemblies, Langmuir, 20 (2004) 7694-7702.

[42] T. Albrecht, A. Guckian, J. Ulstrup, J.G. Vos, Transistor effects and in situ STM of redox molecules at room temperature, IEEE Transactions on Nanotechnology, 4 (2005) 430-434.

[43] T. Albrecht, A. Guckian, J. Ulstrup, J.G. Vos, Transistor-like behavior of transition metal complexes, Nano Lett., 5 (2005) 1451-1455.

[44] C. Li, A. Mishchenko, T. Wandlowski, Charge Transport in Single Molecular Junctions at the Solid/Liquid Interface, in: R.M. Metzger (Ed.) Unimolecular and Supramolecular Electronics II: Chemistry and Physics Meet at Metal-Molecule Interfaces, Springer Berlin Heidelberg, Berlin, Heidelberg, 2012, pp. 121-188.

[45] B. Capozzi, Q. Chen, P. Darancet, M. Kotiuga, M. Buzzeo, J.B. Neaton, C. Nuckolls, L. Venkataraman, Tunable Charge Transport in Single-Molecule Junctions via Electrolytic Gating, Nano Lett., 14 (2014) 1400-1404.

[46] I. Diez-Perez, Z. Li, J. Hihath, J. Li, C. Zhang, X. Yang, L. Zang, Y. Dai, X. Feng, K. Muellen, N. Tao, Gate-controlled electron transport in coronenes as a bottom-up approach towards graphene transistors, Nature Comm., 1 (2010) 31.

[47] R.J. Brooke, C. Jin, D.S. Szumski, R.J. Nichols, B.-W. Mao, K.S. Thygesen, W. Schwarzacher, Single-Molecule Electrochemical Transistor Utilizing a Nickel-Pyridyl Spinterface, Nano Lett., 15 (2015) 275-280.

[48] R.J. Brooke, D.S. Szumski, A. Vezzoli, S.J. Higgins, R.J. Nichols, W. Schwarzacher, Dual Control of Molecular Conductance through pH and Potential in Single-Molecule Devices, Nano Lett., 18 (2018) 1317-1322.

[49] M.F. Crommie, C.P. Lutz, D.M. Eigler, Confinement of Electrons to Quantum Corrals on a Metal-Surface, Science, 262 (1993) 218-220.

[50] T. Tada, K. Yoshizawa, Molecular design of electron transport with orbital rule: toward conductance-decay free molecular junctions, PCCP, 17 (2015) 32099-32110.

[51] N. Darwish, I. Diez-Perez, P. Da Silva, N.J. Tao, J.J. Gooding, M.N. Paddon-Row, Observation of Electrochemically Controlled Quantum Interference in a Single Anthraquinone-Based Norbornylogous Bridge Molecule, Angew. Chem.-Int. Edit., 51 (2012) 3203-3206.

[52] B. Huang, X. Liu, Y. Yuan, Z.-W. Hong, J.-F. Zheng, L.-Q. Pei, Y. Shao, J.-F. Li, X.-S. Zhou, J.-Z. Chen, S. Jin, B.-W. Mao, Controlling and Observing Sharp-Valleyed Quantum Interference Effect in Single Molecular Junctions, J. Am. Chem. Soc., 140 (2018) 17685-17690.

[53] X. Li, Z. Tan, X. Huang, J. Bai, J. Liu, W. Hong, Experimental investigation of quantum interference in charge transport through molecular architectures, J. Mater. Chem. C, 7 (2019) 12790-12808.

[54] Y. Li, M. Buerkle, G. Li, A. Rostamian, H. Wang, Z. Wang, D.R. Bowler, T. Miyazaki, L. Xiang, Y. Asai, G. Zhou, N. Tao, Gate controlling of quantum interference and direct observation of anti-resonances in single molecule charge transport, Nature Mater., 18 (2019) 357-363.

[55] Z. Li, B. Han, G. Meszaros, I. Pobelov, T. Wandlowski, A. Blaszczyk, M. Mayor, Two-dimensional assembly and local redox-activity of molecular hybrid structures in an electrochemical environment, Faraday Discuss., 131 (2006) 121-143.

[56] Z.H. Li, I. Pobelov, B. Han, T. Wandlowski, A. Blaszczyk, M. Mayor, Conductance of redox-active single molecular junctions: an electrochemical approach, Nanotechnology, 18 (2007) 044018.

[57] E. Leary, S.J. Higgins, H. van Zalinge, W. Haiss, R.J. Nichols, S. Nygaard, J.O. Jeppesen, J. Ulstrup, Structure-property relationships in redox-gated single molecule junctions - A comparison of pyrrolo-tetrathiafulvalene and viologen redox groups, J. Am. Chem. Soc., 130 (2008) 12204-12205.

[58] I.V. Pobelovt, Z.H. Li, T. Wandlowski, Electrolyte Gating in Redox-Active Tunneling Junctions-An Electrochemical STM Approach, J. Am. Chem. Soc., 130 (2008) 16045-16054.

[59] B. Han, Z. Li, C. Li, I. Pobelov, G. Su, R. Aguilar-Sanchez, T. Wandlowski, From Self-Assembly to Charge Transport with Single Molecules - An Electrochemical Approach, in: P. Broekmann, K.H. Dotz, C.A. Schalley (Eds.) Templates in Chemistry Iii2009, pp. 181-255.

[60] V. Kolivoska, M. Valasek, M. Gal, R. Sokolova, J. Bulickova, L. Pospisil, G. Meszaros, M. Hromadova, Single-Molecule Conductance in a Series of Extended Viologen Molecules, J. Phys. Chem. Letts., 4 (2013) 589-595.

[61] H.M. Osorio, S. Catarelli, P. Cea, J.B.G. Gluyas, F. Hartl, S.J. Higgins, E. Leary, P.J. Low, S. Martin, R.J. Nichols, J. Tory, J. Ulstrup, A. Vezzoli, D.C. Milan, Q. Zeng, Electrochemical Single-Molecule Transistors with Optimized Gate Coupling, J. Am. Chem. Soc., 137 (2015) 14319-14328.

[62] W. Zhang, S. Gan, A. Vezzoli, R.J. Davidson, D.C. Milan, K.V. Luzyanin, S.J. Higgins, R.J. Nichols, A. Beeby, P.J. Low, B. Li, L. Niu, Single-Molecule Conductance of Viologen–Cucurbit[8]uril Host–Guest Complexes, ACS Nano, 10 (2016) 5212-5220.

[63] B.Q. Xu, X.Y. Xiao, X.M. Yang, L. Zang, N.J. Tao, Large gate modulation in the current of a room temperature single molecule transistor, J. Am. Chem. Soc., 127 (2005) 2386-2387.

[64] X.L. Li, B.Q. Xu, X.Y. Xiao, X.M. Yang, L. Zang, N.J. Tao, Controlling charge transport in single molecules using electrochemical gate, Faraday Discuss., 131 (2006) 111-120.

[65] X. Li, J. Hihath, F. Chen, T. Masuda, L. Zang, N. Tao, Thermally activated electron transport in single redox molecules, J. Am. Chem. Soc., 129 (2007) 11535-11542.

[66] C. Li, A. Mishchenko, Z. Li, I. Pobelov, T. Wandlowski, X.Q. Li, F. Wuerthner, A. Bagrets, F. Evers, Electrochemical gate-controlled electron transport of redox-active single perylene bisimide molecular junctions, J. Phys.: Condens. Matter, 20 (2008) 374122.

[67] C. Li, V. Stepanenko, M.-J. Lin, W. Hong, F. Wuerthner, T. Wandlowski, Charge transport through perylene bisimide molecular junctions: An electrochemical approach, Physica Status Solidi B-Basic Solid State Physics, 250 (2013) 2458-2467.

[68] Y.H. Li, M. Baghernejad, A.G. Qusiy, D.Z. Manrique, G.X. Zhang, J. Hamill, Y.C. Fu, P. Broekmann, W.J. Hong, T. Wandlowski, D.Q. Zhang, C. Lambert, Three-State Single-Molecule

Naphthalenediimide Switch: Integration of a Pendant Redox Unit for Conductance Tuning, Angew. Chem.-Int. Edit., 54 (2015) 13586-13589.

[69] S. Hosseini, C. Madden, J. Hihath, S.Y. Guo, L. Zang, Z.H. Li, Single -Molecule Charge Transport and Electrochemical Gating in Redox-Active Perylene Diimide Junctions, J. Phys. Chem. C, 120 (2016) 22646-22654.

[70] S. Tsoi, I. Griva, S.A. Trammell, A.S. Blum, J.M. Schnur, N. Lebedev, Electrochemically controlled conductance switching in a single molecule: Quinone-modified oligo(phenylene vinylene), ACS Nano, 2 (2008) 1289-1295.

[71] P. Petrangolini, A. Alessandrini, L. Berti, P. Facci, An Electrochemical Scanning Tunneling Microscopy Study of 2-(6-Mercaptoalkyl)hydroquinone Molecules on Au(111), J. Am. Chem. Soc., 132 (2010) 7445-7453.

[72] S. Tsoi, I. Griva, S.A. Trammell, G. Kedziora, J.M. Schnur, N. Lebedev, Observation of two discrete conductivity states in quinone-oligo(phenylene vinylene), Nanotechnology, 21 (2010) 085704.

[73] N. Darwish, I. Diez-Perez, S.Y. Guo, N.J. Tao, J.J. Gooding, M.N. Paddon-Row, Single Molecular Switches: Electrochemical Gating of a Single Anthraquinone-Based Norbornylogous Bridge Molecule, J. Phys. Chem. C, 116 (2012) 21093-21097.

[74] F. Chen, J. He, C. Nuckolls, T. Roberts, J.E. Klare, S. Lindsay, A molecular switch based on potential-induced changes of oxidation state, Nano Lett., 5 (2005) 503-506.

[75] B.Q.Q. Xu, X.L.L. Li, X.Y.Y. Xiao, H. Sakaguchi, N.J.J. Tao, Electromechanical and conductance switching properties of single oligothiophene molecules, Nano Lett., 5 (2005) 1491-1495.

[76] I. Visoly-Fisher, K. Daie, Y. Terazono, C. Herrero, F. Fungo, L. Otero, E. Durantini, J.J. Silber, L. Sereno, D. Gust, T.A. Moore, A.L. Moore, S.M. Lindsay, Conductance of a biomolecular wire, PNAS, 103 (2006) 8686-8690.

[77] J. He, F. Chen, S. Lindsay, C. Nuckolls, Length dependence of charge transport in oligoanilines, Appl. Phys. Lett., 90 (2007) 072112.

[78] T. Morita, S. Lindsay, Reduction-induced switching of single-molecule conductance of fullerene derivatives, J. Phys. Chem. B, 112 (2008) 10563-10572.

[79] X.Y. Xiao, L.A. Nagahara, A.M. Rawlett, N.J. Tao, Electrochemical gate-controlled conductance of single oligo(phenylene ethynylene)s, J. Am. Chem. Soc., 127 (2005) 9235-9240.

[80] J. He, Q. Fu, S. Lindsay, J.W. Ciszek, J.M. Tour, Electrochemical origin of voltage-controlled molecular conductance switching, J. Am. Chem. Soc., 128 (2006) 14828-14835.

[81] Z. Li, H. Li, S. Chen, T. Froehlich, C. Yi, C. Schoenenberger, M. Calame, S. Decurtins, S.-X. Liu, E. Borguet, Regulating a Benzodifuran Single Molecule Redox Switch via Electrochemical Gating and Optimization of Molecule/Electrode Coupling, J. Am. Chem. Soc., 136 (2014) 8867-8870.

[82] Q.J. Chi, O. Farver, J. Ulstrup, Long-range protein electron transfer observed at the single-molecule level: In situ mapping of redox-gated tunneling resonance, PNAS, 102 (2005) 16203-16208.

[83] A. Alessandrini, M. Salerno, S. Frabboni, P. Facci, Single-metalloprotein wet biotransistor, Appl. Phys. Lett., 86 (2005) 133902.

[84] Q.J. Chi, J.D. Zhang, P.S. Jensen, H.E.M. Christensen, J. Ulstrup, Long-range interfacial electron transfer of metalloproteins based on molecular wiring assemblies, Faraday Discuss., 131 (2006) 181-195.

[85] J. Hihath, F. Chen, P.M. Zhang, N.J. Tao, Thermal and electrochemical gate effects on DNA conductance, J. Phys.: Condens. Matter, 19 (2007) 215202.

[86] Q.J. Chi, J.D. Zhang, T. Arslan, L. Borg, G.W. Pedersen, H.E.M. Christensen, R.R. Nazmutdinov, J. Ulstrup, Approach to Interfacial and Intramolecular Electron Transfer of the Diheme Protein Cytochrome c(4) Assembled on Au(111) Surfaces, J. Phys. Chem. B, 114 (2010) 5617-5624.

[87] V. Climent, J.D. Zhang, E.P. Friis, L.H. Ostergaard, J. Ulstrup, Voltammetry and Single-Molecule in Situ Scanning Tunneling Microscopy of Laccases and Bilirubin Oxidase in Electrocatalytic Dioxygen Reduction on Au(111) Single-Crystal Electrodes, J. Phys. Chem. C, 116 (2012) 1232-1243.

[88] J.D. Zhang, Q.J. Chi, A.G. Hansen, P.S. Jensen, P. Salvatore, J. Ulstrup, Interfacial electrochemical electron transfer in biology - Towards the level of the single molecule, FEBS Letters, 586 (2012) 526-535.

[89] P. Salvatore, D.D. Zeng, K.K. Karlsen, Q.J. Chi, J. Wengel, J. Ulstrup, Electrochemistry of Single Metalloprotein and DNA-Based Molecules at Au(111) Electrode Surfaces, Chemphyschem, 14 (2013) 2101-2111.

[90] A.G. Hansen, P. Salvatore, K.K. Karlsen, R.J. Nichols, J. Wengel, J. Ulstrup, Electrochemistry and in situ scanning tunnelling microscopy of pure and redox-marked DNA- and UNA-based oligonucleotides on Au(111)-electrode surfaces, PCCP, 15 (2013) 776-786.

[91] L.M. Xiang, J.L. Palma, Y.Q. Li, V. Mujica, M.A. Ratner, N.J. Tao, Gate-controlled conductance switching in DNA, Nature Comm., 8 (2017) 14471.

[92] R.A. Wassel, G.M. Credo, R.R. Fuierer, D.L. Feldheim, C.B. Gorman, Attenuating Negative Differential Resistance in an Electroactive Self-Assembled Monolayer-Based Junction, J. Am. Chem. Soc., 126 (2004) 295-300.

[93] X.Y. Xiao, D. Brune, J. He, S. Lindsay, C.B. Gorman, N.J. Tao, Redox-gated electron transport in electrically wired ferrocene molecules, Chem. Phys., 326 (2006) 138-143.

[94] T. Albrecht, K. Moth-Poulsen, J.B. Christensen, A. Guckian, T. Bjornholm, J.G. Vos, J. Ulstrup, In situ scanning tunnelling spectroscopy of inorganic transition metal complexes, Faraday Discuss., 131 (2006) 265-279.

[95] T. Albrecht, A. Guckian, A.M. Kuznetsov, J.G. Vos, J. Ulstrup, Mechanism of electrochemical charge transport in individual transition metal complexes, J. Am. Chem. Soc., 128 (2006) 17132-17138.

[96] T. Albrecht, K. Moth-Poulsen, J.B. Christensen, J. Hjelm, T. Bjornholm, J. Ulstrup, Scanning tunneling spectroscopy in an ionic liquid, J. Am. Chem. Soc., 128 (2006) 6574-6575.

[97] K. Seo, A.V. Konchenko, J. Lee, G.S. Bang, H. Lee, Molecular conductance switch-on of single ruthenium complex molecules, J. Am. Chem. Soc., 130 (2008) 2553-2559.

[98] A.M. Ricci, E.J. Calvo, S. Martin, R.J. Nichols, Electrochemical Scanning Tunneling Spectroscopy of Redox-Active Molecules Bound by Au-C Bonds, J. Am. Chem. Soc., 132 (2010) 2494-2495.

[99] Z. Li, Y. Liu, S.F.L. Mertens, I.V. Pobelov, T. Wandlowski, From Redox Gating to Quantized Charging, J. Am. Chem. Soc., 132 (2010) 8187-8193.

[100] J.J. Davis, B. Peters, W. Xi, J. Appel, A. Kros, T.J. Aartsma, R. Stan, G.W. Canters, Large Amplitude Conductance Gating in a Wired Redox Molecule, J. Phys. Chem. Letts., 1 (2010) 1541-1546.

[101] S. Chappell, C. Brooke, R.J. Nichols, L.J. Kershaw Cook, M. Halcrow, J. Ulstrup, S.J. Higgins, Evidence for a hopping mechanism in metal|single molecule|metal junctions involving conjugated metal–terpyridyl complexes; potential-dependent conductances of

complexes [M(pyterpy)2]2+ (M = Co and Fe; pyterpy = 4’-(pyridin-4-yl)-2,2’:6’,2’’-terpyridine) in ionic liquid, Faraday Discuss., 193 (2016) 113-131.

[102] Y.Q. Li, H. Wang, Z.X. Wang, Y.J. Qiao, J. Ulstrup, H.Y. Chen, G. Zhou, N.J. Tao, Transition from stochastic events to deterministic ensemble average in electron transfer reactions revealed by single-molecule conductance measurement, PNAS, 116 (2019) 3407-3412.

[103] S. Guo, J. Manuel Artes, I. Diez-Perez, Electrochemically-gated single-molecule electrical devices, Electrochim. Acta, 110 (2013) 741-753.

[104] C.L. Wu, X.H. Qiao, C.M. Robertson, S.J. Higgins, C.X. Cai, R.J. Nichols, A. Vezzoli, A Chemically Soldered Polyoxometalate Single-Molecule Transistor, Angew. Chem.-Int. Edit., 59 (2020) 12029-12034.

[105] X.-S. Zhou, L. Liu, P. Fortgang, A.-S. Lefevre, A. Serra-Muns, N. Raouafi, C. Amatore, B.-W. Mao, E. Maisonhaute, B. Schoellhorn, Do Molecular Conductances Correlate with Electrochemical Rate Constants? Experimental Insights, J. Am. Chem. Soc., 133 (2011) 7509-7516.

[106] T. Hines, I. Diez-Perez, H. Nakamura, T. Shimazaki, Y. Asai, N. Tao, Controlling Formation of Single-Molecule Junctions by Electrochemical Reduction of Diazonium Terminal Groups, J. Am. Chem. Soc., 135 (2013) 3319-3322.

[107] T.C. Ting, L.Y. Hsu, M.J. Huang, E.C. Horng, H.C. Lu, C.H. Hsu, C.H. Jiang, B.Y. Jin, S.M. Peng, C.H. Chen, Energy-Level Alignment for Single-Molecule Conductance of Extended Metal-Atom Chains, Angew. Chem.-Int. Edit., 54 (2015) 15734-15738.

[108] N. Ferri, N. Algethami, A. Vezzoli, S. Sangtarash, M. McLaughlin, H. Sadeghi, C.J. Lambert, R.J. Nichols, S.J. Higgins, Hemilabile Ligands as Mechanosensitive Electrode Contacts for Molecular Electronics, Angew. Chem.-Int. Edit., 58 (2019) 16583-16589.

[109] E. Leary, G. Kastlunger, B. Limburg, L. Rincon-Garcia, J. Hurtado-Gallego, M.T. Gonzalez, G.R. Bollinger, N. Agrait, S.J. Higgins, H.L. Anderson, R. Stadler, R.J. Nichols, Long-lived charged states of single porphyrin-tape junctions under ambient conditions, Nanoscale Horizons, 6 (2021) 49-58.

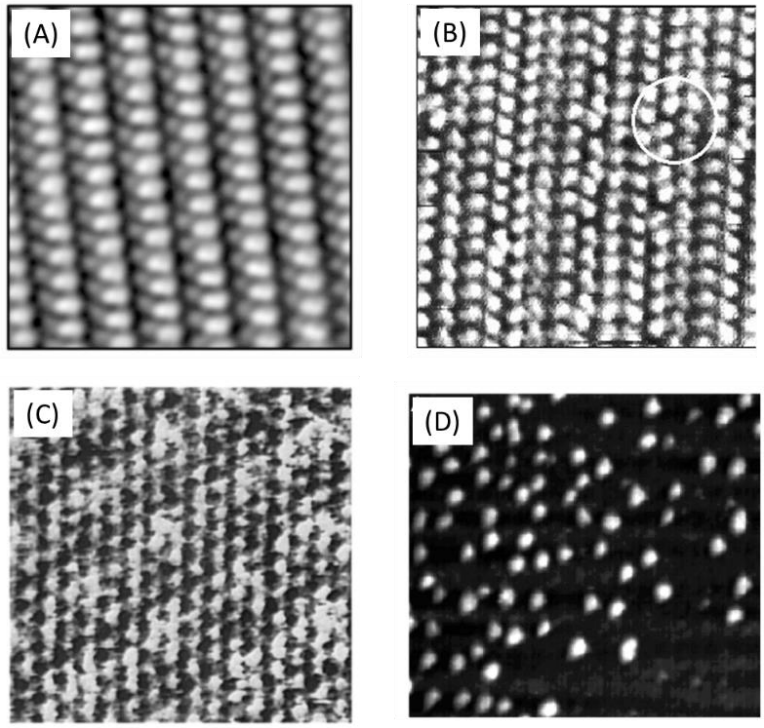

Figure 1. Four selected examples of high-resolution images recorded by in-situ electrochemical STM. (a) 7 x 7 nm^2 area of an ordered (bi)sulfate layer on Au(100) electrode in 0.1 M H_2SO_4 at 0.35 V, (b) 8 x 8 nm^2 image of thymine chemisorbed on Au(111) recorded at 0.7 V in 10 mM thymine + 10 mM $HClO_4$. The circle highlights a stacking defect in the 2D molecular layer, (c) 5 x 5 nm^2 image of an underpotentially deposited Cu adlayer on Au(111) in 0.1M $HClO_4$ + 0.01 M $Cu(ClO_4)_2$ solution containing small amounts of $C1^-$(aq.) at 0.25 V, (d) 100 x 100 nm^2 image of yeast cytochrome adsorbed on Au(111) at -0.16 V in 10 mM phosphate buffer, pH 7.5. All working electrode potentials versus SCE. Fig. 1a reprinted from ref. [10], copyright 1999, with permission from Elsevier, Fig. 1b reprinted with permission from ref. [11] ,copyright 1999 American Chemical Society, Fig. 1c reprinted from ref. [12], copyright 1995, with permission from Elsevier, Fig. 1d reprinted with permission from ref. [13], copyright 2003 American Chemical Society.

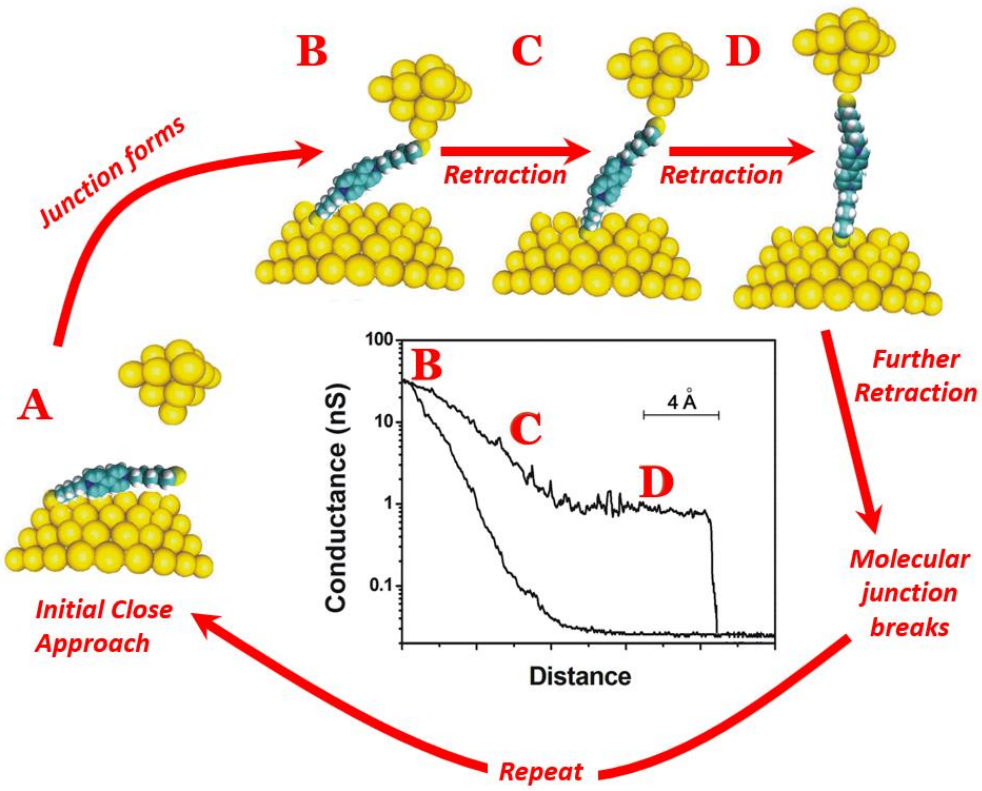

Figure 2. A schematic illustration on the *I*(*s*) method[15] which uses an STM to form molecular junctions. Molecular junction formation occurs between A and B which is followed by STM tip retraction until the molecular junction cleaves after D. Corresponding conductance versus retraction distance curves are shown in the panel, for two situations: molecular junction formation (upper curve with a plateau) and no molecular junction formation (lower curve with a plain exponential decay). Adapted from ref. [16] with permission from the PCCP Owner Societies.

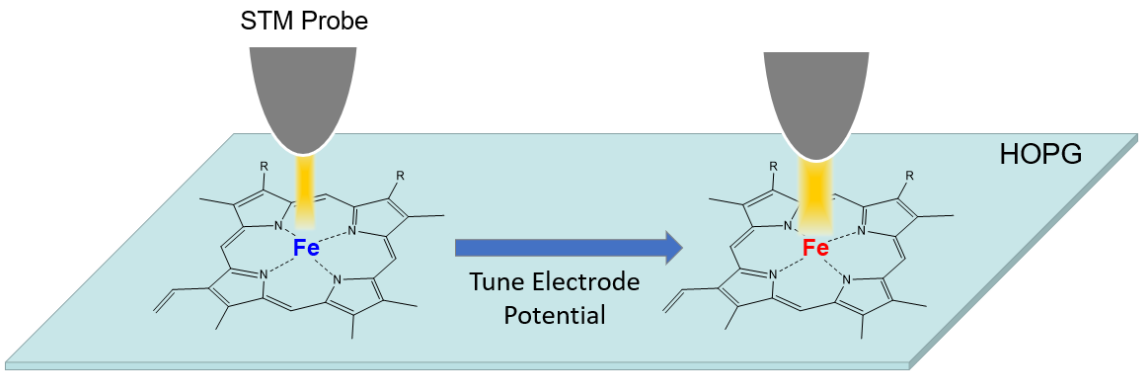

Figure 3. The principle of electrochemical scanning tunnelling spectroscopy (EC-STS) illustrated schematically with the example of an iron porphyrin complex adsorbed on a highly oriented pyrolytic graphite (HOPG) substrate, as developed by N.J. Tao.[24] The electrode potential can be tuned to enhance tunnelling current through the adsorbate as illustrated and this can be used to study mechanisms of single-molecule junction electronic conductivity at electrode-electrolyte interfaces.

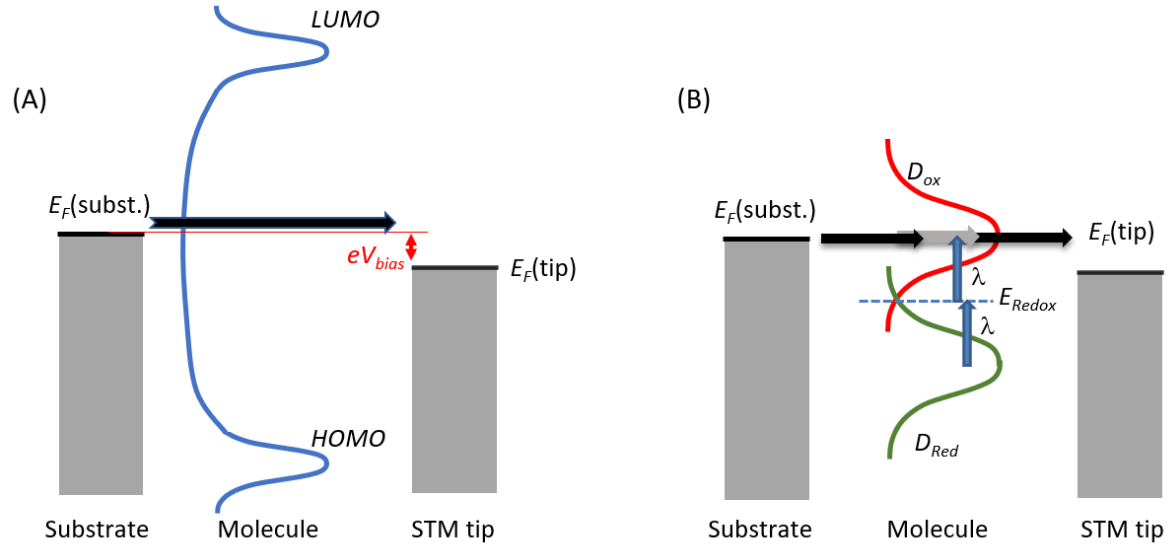

Figure 4. Illustrations of coherent tunnelling through a molecular bridge (A) and resonant tunnelling (B) between a metal substrate and STM tip. The coherent tunnelling is illustrated at mid gap conditions with the LUMO and HOMO frontier molecular orbitals relatively distant from the Fermi levels of the substrate and STM tip, E_F(subst.) and E_F(tip), respectively. (B) illustrates resonant tunnelling through the unoccupied (oxidated) state and shows the distribution of empty oxidised (D_{ox}) and occupied reduced (D_{red}) states, the redox potential (E_{Redox}) and reorganisation energy (λ).

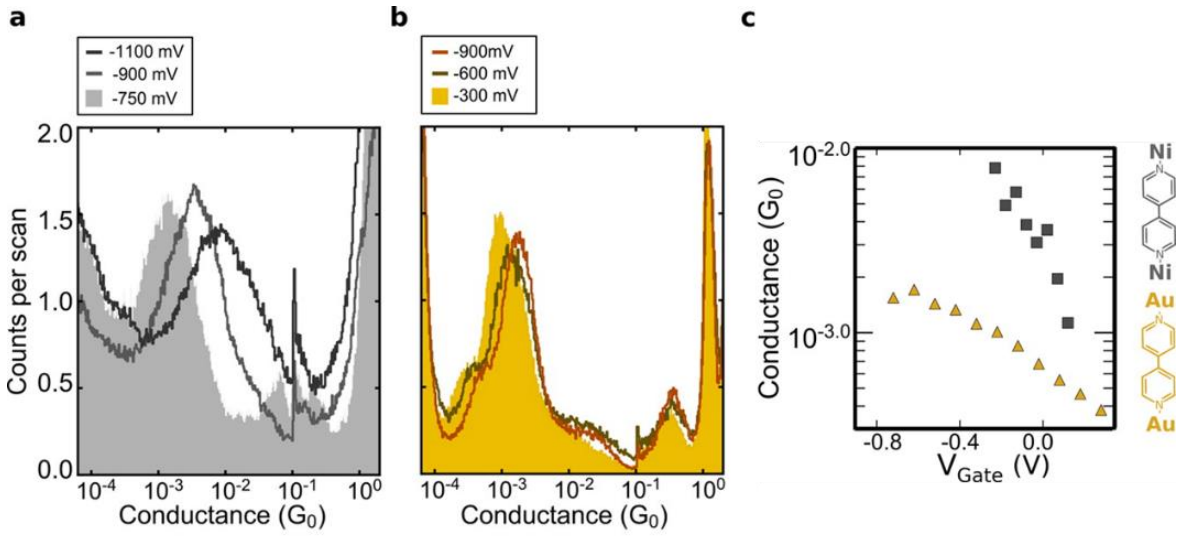

Figure 5. Conductance histograms recorded for (a) Ni-44'BPy-Ni and (b) Au-44'BPy-Au single-molecule junctions at the marked electrode potentials versus a polypyrrole (PPy) quasi-reference electrode (PPy = +0.31 V vs SCE). (c) Experimental conductance values for Ni-44'BPy-Ni (grey) and Au-44'BPy-Au (yellow) junctions versus the electrochemical gating voltage. Data recorded in a pH 3 0.05 M Na_2SO_4 aqueous electrolyte. Reprinted with permission from ref. [47]. Copyright 2015 American Chemical Society.

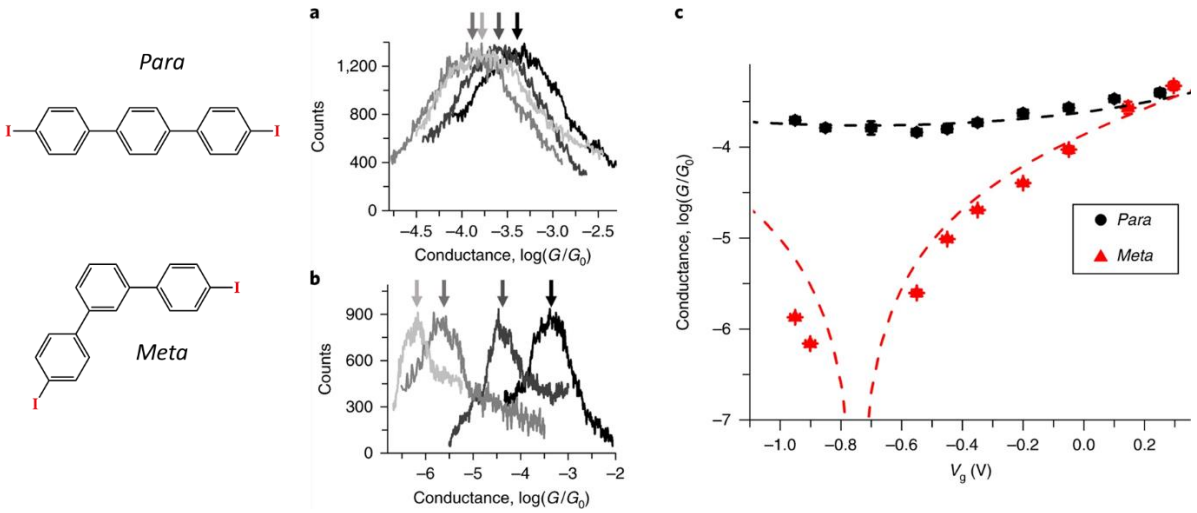

Figure 6. Left: The *Para* and *Meta* single molecular wires. Centre: (a) Conductance histograms of *Para* recorded at different electrolyte gating voltages (V_g) of +0.25, −0.2, −0.55 and −0.95 V (black, dark grey, grey and light grey, respectively), (b) Conductance histograms of *Meta* measured at different electrolyte gating voltages of +0.295 V, −0.2 V, −0.55 V and −0.95 V (black, dark grey, grey and light grey, respectively). Right: (c) The dependence of the average conductance of *Para* (black circles) and *Meta* (red symbols) single molecule wires with the electrochemical gating voltage (V_g). The meta molecular wire shows a sharp destructive interference valley. Reprinted by permission from Springer Nature: Nature Materials, ref. [54] copyright 2019.

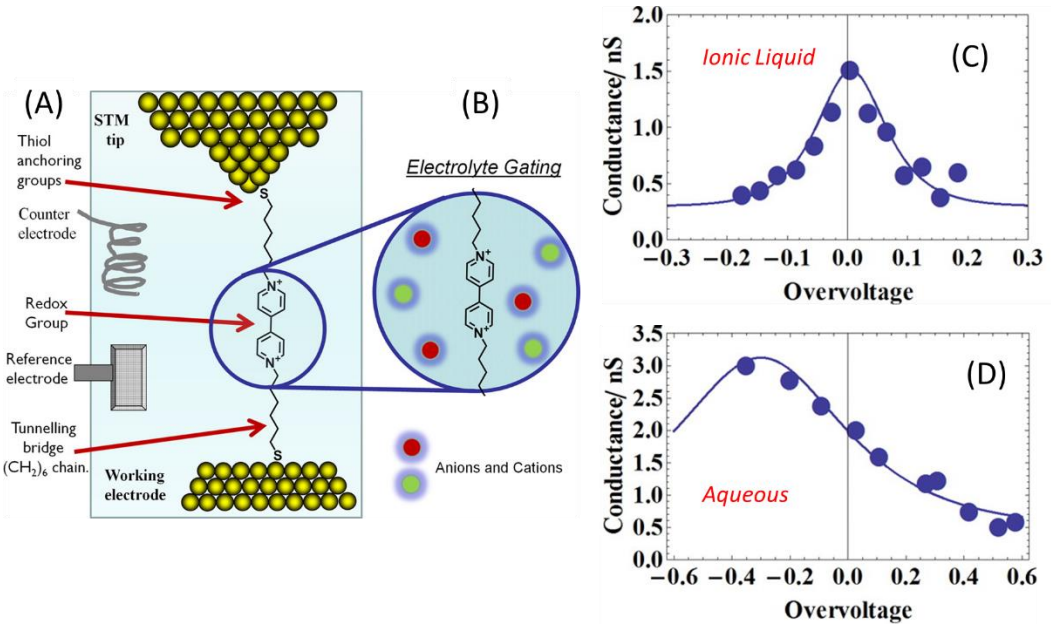

Figure 7. (A) and (B) A viologen (6V6) molecular junction formed between a gold STM tip and a substrate electrode in an bipotentiostat controlled electrochemical STM cell. (C) & (D) single molecule conductance versus electrode potential of the viologen (6V6) single molecule bridge (blue circles) and fitting with the KU model (solid blue lines); (C) is conductance data for an ionic liquid electrolyte, while (D) is for an aqueous electrolyte. Adapted from ref. [61]. Copyright 2015 American Chemical Society.

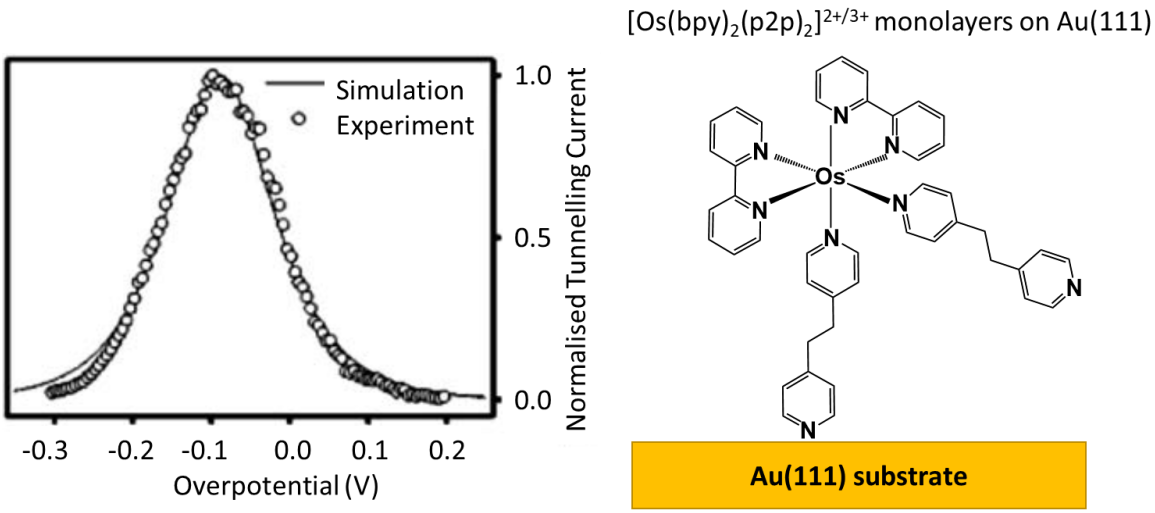

Figure 8. EC-STS of $[Os(bpy)_2(p2p)_2]^{2+/3+}$ monolayers on Au(111) in 0.1 M $HClO_4$ (left) and molecular complex adsorbed on Au(111) (right). The plot shows the normalised STM current versus the overpotential, with this data recorded for V_{bias} = 0.15 V. The simulated data is to the 2-step ET mechanism of Kuzentsov and Ulstrup in the adiabatic limit. Adapted with permission from ref. [43]. Copyright 2005 American Chemical Society.

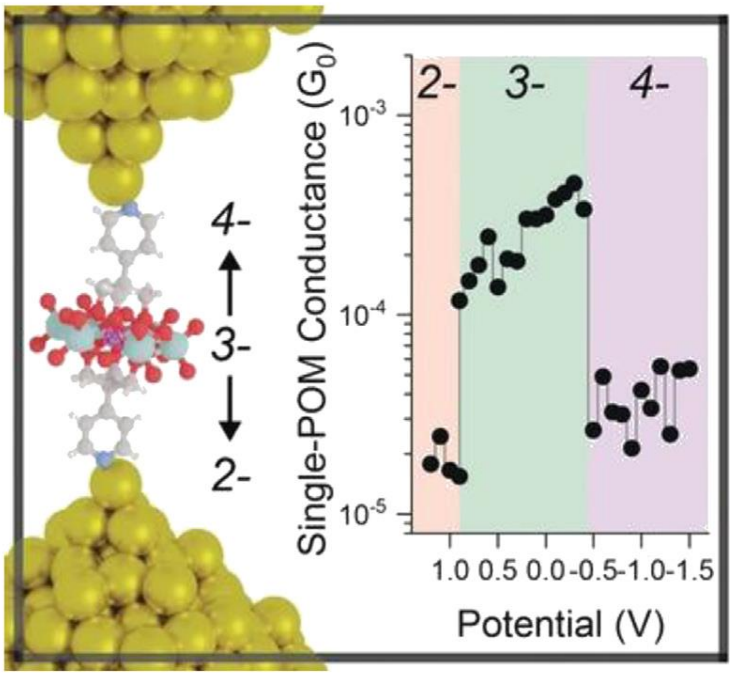

Figure 9. Left: a single molecular wire with an integral polyoxometalate cluster (with 7 metal atoms) attached between a Au STM tip and substrate through pyridyl anchoring groups. Right: single molecular conductance versus electrode potential, showing molecular conductance transitions on switching between differing charge states ($2^- \leftrightarrow 3^- \leftrightarrow 4^-$). Reprinted from reference [104].